High-Resolution Solid-State NMR in Liquids. 2.[1] ^{27}Al NMR Study of AlF_3 Ultrafine Particles

Naoki Satoh[†] and Keisaku Kimura*[,‡]

Contribution from the Kao Institute for Fundamental Research, 1334 Minato Wakayama, Wakayama 640, Japan, and Instrument Center, Institute for Molecular Science, Myodaiji, Okazaki, Aichi 444, Japan. *Received August 28, 1989*

Abstract: High-resolution ^{27}Al nuclear magnetic resonance spectra of AlF_3 ultrafine particles (UFPs) were obtained by means of motional narrowing caused by Brownian motion of UFPs in a liquid phase. The NMR observed spectra can be resolved in five signals at 10, -5, -8, -12, and -16 ppm with respect to an $Al^{3+}(H_2O)_6$ standard. The UFPs were fractionated according to their sizes by using an ultrafiltration technique. From the NMR measurements of fractionated colloidal solutions, the five peaks were classified into three groups by their origins, viz. the peak at -16 ppm is from larger UFPs (diameter D; 9 nm), those at -5, -8, and -12 ppm from smaller UFPs ($1 < D < 3$ nm), while that at 10 ppm from free ions. Line widths of the larger and smaller UFPs were about 10 and 4 ppm (i.e., 1 and 0.4 kHz), respectively. The observed line widths were considerably larger than the calculated values taking into account only dipole–dipole interactions. The quadrupole interaction was suggested to be the origin of this discrepancy. Further, the signal at -8 ppm was assigned to aluminum ions at the surface of the UFPs. The size dependence of chemical shifts is ascribable to change in the degree of ionicity of Al–F bonds, which is a function of the particle size. This interpretation is in agreement with the results of X-ray photoelectron spectroscopy.

NMR lines of solid-state samples are, in general, quite broad due to various reasons such as dipole–dipole interaction, anisotropy of chemical shifts, etc. Rapid and random motion of nuclei suppress these broadening effects, which is well-known as motional narrowing. Brownian motion of ultrafine particles (UFPs) in a liquid phase is, therefore, expected to provide high-resolution NMR spectra for solid-state samples (UFP NMR).[1] Structures and functions of proteins and enzymes, many of which can be classified as UFPs by their sizes, have already been intensively investigated by means of NMR in a liquid phase.[2] The applications of NMR in protein and polymer science indicate a possibility of UFP NMR for studying solid-state samples. However, few attempts have been made in the use of motional narrowing for observing high-resolution solid-state NMR. The "UFP NMR" method is highly advantageous for obtaining an "in situ" information concerning solid surfaces without the need of a high vacuum condition as required in most other techniques and is expected to yield novel information on fundamental phenomena concerning solid surfaces in liquid phases, such as catalysts, dissolution, crystallization, adsorption, etc. Furthermore, UFP NMR is applicable for high-resolution solid-state magnetic resonance of nuclei surrounded by homogeneous abundant spins. There have been two conventional techniques for obtaining high-resolution solid-state NMR spectra, viz. magic angle sample spinning (MAS-NMR) with decoupling of dipole–dipole interactions and those based on multi-pulse sequences. However, satisfactory resolution has not yet been obtained by the use of these techniques for the solid-state NMR of protons. The UFP NMR is expected to effectively narrow the broadened NMR signals of solids irrespective their origin.

We report here on the versatility of the UFP NMR method from aspects of a high-resolution solid-state NMR in abundant spins and a surface NMR. ^{27}Al NMR signals of aluminum fluoride UFPs are observed to be narrowed when UFPs were dispersed in methanol, and an NMR signal from the surfaces of UFPs was obtained. AlF_3 was chosen for demonstrating the effectiveness of UFP NMR, since each ^{27}Al nucleus in AlF_3 is surrounded by six ^{19}F nuclei resulting in very strong dipole–dipole interactions comparable with that of protons. AlF_3 is also well suited for preparing UFP by means of a gas evaporation technique because of its sufficiently high vapor pressure required for sublimation, and its stability with respect to heat treatment and handling in air. The interpretation of ^{27}Al NMR spectra of AlF_3 is also straightforward as there are no structural polymorphs or allotropic forms.

Experimental Section

Sample Preparation and Fractionation. GR grade anhydrous AlF_3 (Katayama Chemical Industries) was used without further purification. AlF_3 UFPs were prepared and dispersed in methanol by the gas flow–cold trap method[3] as shown schematically in Figure 1. The chamber was evacuated by a rotary pump prior to the introduction of Ar gas. A constant flow of Ar gas (pressure = 30 Torr) was introduced from the front of a heater, providing a surrounding gas and a carrier gas. The heater was surrounded by a glass cover in order to develop recoveries of UFPs. AlF_3 powder set in a molybdenum boat was heated, giving a formation of UFPs into a gas stream. The UFPs produced and Ar gas were led to the trap cooled by liquid N_2 with methanol vaporized into the gas stream from the chamber. After the accumulation of a sufficient amount of UFPs, the matrix was melted to obtain colloidal dispersion. The sample of UFPs deposited on the glass cover around the heater was used as a reference sample of powder UFPs against dispersed UFPs. The UFPs or ions were separated according to their sizes by means of an ultrafiltration technique[4] keeping UFPs in a colloidal dispersion state. Ultrafiltration membranes of polysaccharide, YM100, and YM5 (Amicon Co.) were used. Effective pore sizes in methanol are 1 nm < YM5 < YM100 < 3 nm.

^{27}Al NMR and XPS. ^{27}Al NMR measurements on liquid samples were carried out on a conventional FT NMR spectrometer, JEOL GX400 employing a frequency of 104.2 MHz, other conditions being altered according to the purpose of measurements. Colloidal solutions and UFP powder samples were sealed in conventional 10-mm sample tubes. MAS ^{27}Al NMR spectra of bulk AlF_3 were obtained by employing sample spinning rates of 8.1 and 3.0 kHz and by using $Al[H_2O]_6^{3+}$ as an external standard of chemical shifts throughout all measurements. Longitudinal relaxation time T_1 was measured by an inversion recovery method with the 180°, τ, 90° pulse sequence. All measurements were carried out at room temperature.

XPS measurements were carried out on a VG Scientific ESCALAB MKII spectrometer employing AlK_α (1486.6 ev) line for X-ray excitation. All samples except the bulk one were prepared by depositing and drying UFP colloidal solutions on a Ni stage. The bulk sample was fixed on a Ni stage using an adhesive tape.

Observations by a Transmission Electron Microscope. The shapes and sizes by UFPs were determined on a Hitachi H-500H transmission electron microscope (TEM) at the laboratory of electron microscopy, the

[†] Kao Institute for Fundamental Research.
[‡] Institute for Molecular Science.

(1) The first paper of this series: Kimura, K.; Satoh, N. *Chem. Lett.* **1989**, 271-274.
(2) Dwek, R. A. *Nuclear Magnetic Resonance in Biochemistry*; Oxford University Press: London, 1973.
(3) Kimura, K.; Bandow, S. *Bull. Chem. Soc. Jpn.* **1983**, *56*, 3578-3584.
(4) For example: *Method in Enzymology XXII*; Jakoby, W. B.; Ed.; Academic Press: New York, San Francisco, London, 1971; p 44.

0002-7863/90/1512-4688$02.50/0 © 1990 American Chemical Society

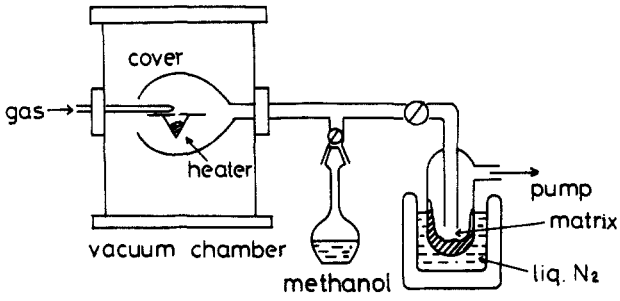

Figure 1. The apparatus for the gas flow-cold trap method.

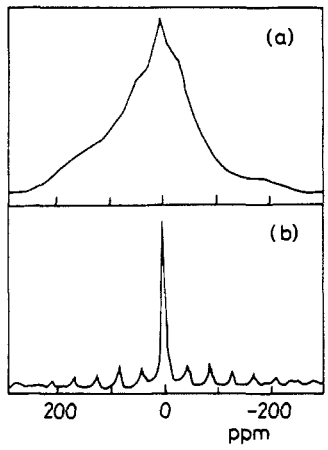

Figure 2. MAS ^{27}Al NMR spectra of bulk samples of (a) AlF_3 and (b) $AlCl_3$. The sample spinning rate was 3 kHz.

National Institute for Physiological Science, Okazaki. Specimens for TEM were prepared by dropping sample solutions on Cu grids coated by a carbon film with 8-nm thickness.

Results

Confirmation of Motional Narrowing. The MAS ^{27}Al NMR spectra of bulk samples of AlF_3 and $AlCl_3$ measured under similar conditions (Figure 2) show that while the NMR line of $AlCl_3$ is sharp, that of AlF_3 is considerably broad. Figure 3a shows a ^{27}Al NMR spectrum of a powder sample of AlF_3 UFPs measured with a 10° pulse, 25 μs delay time. Observed line width was about 7.2 kHz. Figure 3b shows a spectrum from a UFP/methanol colloidal dispersion under the same condition as that for powder UFPs. The line width is 2.3 kHz. Furthermore, several fine structures are found. Since an elongation of delay time suppresses the intensities of the broader lines (shorter T_2), conditions were changed to a 45° pulse and 200 μs delay time in order to observe each of the peaks more separately. Figure 4a is a spectrum from the same sample as that in Figure 3b observed after an alternation of the pulse conditions. All peaks remained in the same resonance position after this alternation of the conditions. Two shoulders (1 and 2) and three peaks (3, 4, and 5) were clearly observed. The intensity of peak 5 is lowered after the change of pulse conditions.

UFPs made by the gas evaporation techniques have a size distribution, the width of which is roughly the same as its mean diameter.[5] To observe the effect of particle size on the position and width of NMR lines, fine particles were fractionated by their sizes by using ultrafiltration membranes. Figure 4b shows a spectrum from a component which did not pass a YM100 membrane. This colloidal solution is labeled by NP100. The peaks 3 and 5 are obvious. This main peak, 5, has a width of about 0.99 kHz. Figure 5a shows a TEM picture of the deposited sample of NP100. Fine particles with a diameter of ca. 10 nm and somewhat irregular shapes are observed. The X-ray diffraction measurement of concentrated NP100 solution gives only a broad (011) reflection. From the Scherrer's equation relating the width

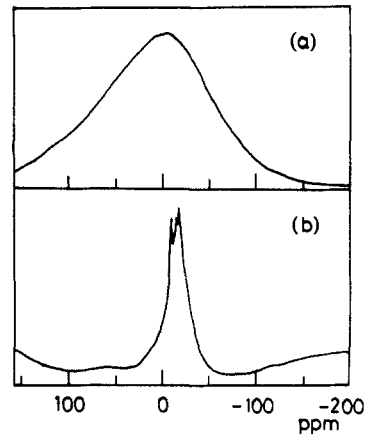

Figure 3. ^{27}Al NMR spectra of AlF_3 UFP (a) powder sample and (b) colloidal dispersion sample measured with a conventional FT NMR spectrometer for liquid samples. Both measurements were carried out with conditions of 10° pulse, 25 μs delay time and 5000 times scans.

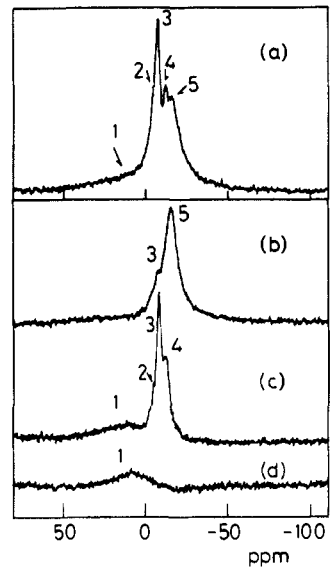

Figure 4. ^{27}Al NMR spectra of AlF_3 UFP/methanol dispersion measured after the alternation of pulse conditions. The pulse width and the delay time were changed to 45° and 200 μs from the conditions in Figure 3. The spectra were from (a) an original colloidal solution which is the same as Figure 3b, (b) an NP100 colloidal solution including larger particles which did not pass a YM100 ultrafiltration membrane (3-nm pore size in methanol), (c) a P100 colloidal solution including smaller particles which pass a YM100, and (d) a P5 solution including complex ions which pass a YM5 (1-nm pore size in methanol).

of a reflection to the size of crystallites,[6] the mean diameter of UFPs of NP100 is obtained to be 9.3 nm, just corresponding to the TEM observations. An interplaner spacing of (011) direction was found to be shortened by ca. 1%. Figure 4 (parts c and d) are the spectra from UFPs of effluents from a YM100 and a YM5 membrane labeled as P100 and P5, respectively. The peak 1 was observed in all spectra from UFP colloidal solution with the identical intensity except Figure 4b which was measured just after the separation. Slight but clear scattering light was observed by an irradiation of He–Ne laser from the colloid solution of P100 in a dark condition, whereas no scattering light was observed from the P5 solution. Figure 5b shows the TEM image of the deposits from a colloidal solution of P100 exhibiting UFPs with irregular shapes and diameters of ca. 3 nm. Figure 6 shows changes of NMR spectra induced by the addition of water from the colloidal solutions in stationary states. The decrease in intensities of peak 3 is observed at the expense of an appearance of low field peaks after the addition of H_2O to 4.5 vol. %, whereas no changes are

(5) Kimura, K. *Bull. Chem. Soc. Jpn.* **1987**, *60*, 3093–3097.

(6) Wilson, A. J. C. *X-ray Optics*, 2nd ed.; Methuen: London, 1962.

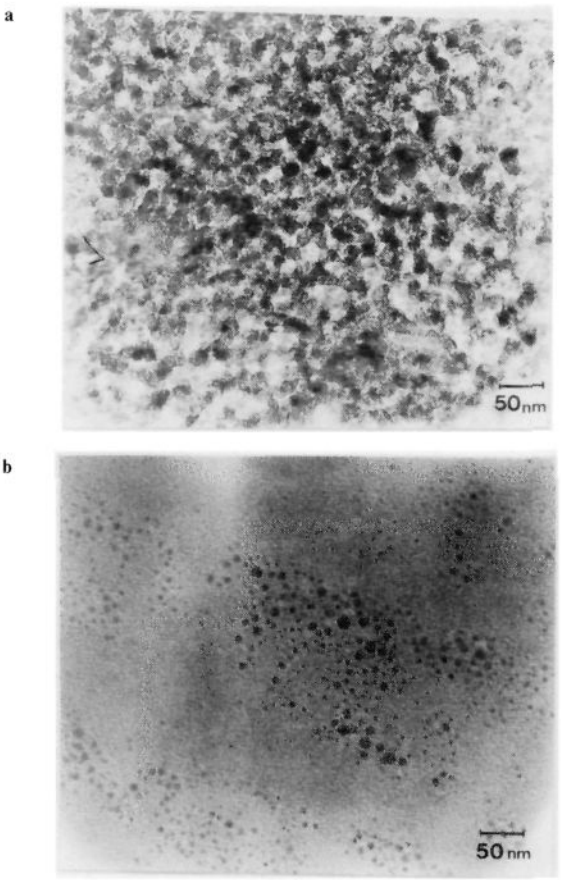

Figure 5. TEM micrograph of AlF_3 UFPs deposited from (a) NP100 and (b) P100 colloidal solutions.

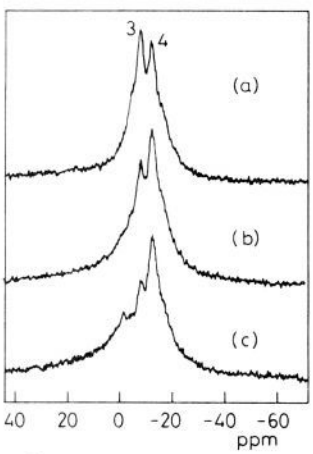

Figure 6. Change of ^{27}Al NMR spectra with the addition of water. The colloidal solution used was an original solution which was in a stationary state. The spectra were from the colloidal solutions of (a) water free, (b) 4.5 vol % water, and (c) 8.7 vol % water. The measurement conditions are as for Figure 4.

observed in peak 4. After the additional amount of H_2O up to 8.7 vol %, a new peak is observed at −1.5 ppm.

Time Dependence of NMR Signals. The relative intensities of NMR signals from an original AlF_3 UFPs/methanol colloidal solution was found to change with time. Peaks 1 and 5 are dominantly observed, while peaks 2 and 3 are observed as shoulders just after the sample preparation. Subsequently intensity of peak 5 decreases at the expense of the gradual increase of peaks 3 and 4, whereas peak 1 does not change its intensity during this period. It took more than 40 days to reach a stationary state. Finally peak 5 disappears, and at the same time the intensity of peak 4 becomes comparable to peak 3. The large UFPs are observed in

Table I. NMR Data of AlF_3 UFP Dispersion

peak no.	1	2	3	4	5
chemical shift (ppm)	10	−5	−8	−12	−16
peak width (kHz)	2.5		0.42	0.63	0.99
T_1 (ms)			1.0	2.45	
T_2 (ms)	0.13		0.76	0.51	0.32
diameter (D) of UFP (nm)	$D < 1$	$1 < D < 3$	surface	$1 < D < 3$	$D \sim 10$

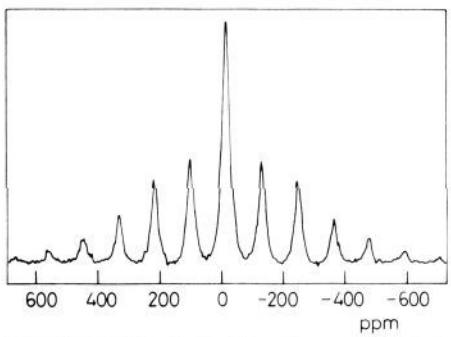

Figure 7. MAS ^{27}Al NMR of bulk AlF_3 with a sample spinning rate of 8.1 kHz. The main peak is located at −16 ppm.

NP100 solution (Figure 5a) were not observed in a solution in the stationary state by TEM. All measurements and analyses except the measurements of T_1 and the measurements of the effect of additives were performed 4 days after the preparation of original solutions. At this time, all NMR signals from the peaks 1–5 were observed with sufficient intensities. Figure 6a thus shows the spectrum of the solution which comes to a stationary state. The results of chemical shifts, line widths, etc. are all summarized in Table I.

Discussion

Assignment. The NMR spectra (Figure 4d) of the effluent from YM5 membrane (nominal pore size 1 nm) is exactly the same as that observed from a saturated AlF_3 solution of methanol which is known to contain Al^{3+} ions. Peak 1 is, therefore, assigned to the signal from aluminum ions in methanol. Further, this peak was always observed in all fractions of UFP colloidal solution with the identical intensity except in that measured just after the separation (cf. Figure 4b). This finding suggests that surfaces of AlF_3 UFPs come to the dissolution equilibrium with ions. The signals 2, 3, and 4 arise from the UFPs with a size ranging from 1 to 3 nm. More than half of Al atoms (ions) exist on the surfaces of such UFPs and are very sensitive to external effects so that the NMR line shape can change by active additives. The drastic reduction in intensity of peak 3 upon addition of water (cf. Figure 6) suggests that this peak arises from surfaces of the UFPs. Furthermore, very slow time-dependent phenomenon was observed as for peaks 3, 4, and 5. At the initial stage, the dominant peak 5 gradually decreased and finally disappeared, whereas peaks 3 and 4 increased slowly. There are no larger UFPs as revealed by the TEM measurement (cf. Figure 5a), which suggests that larger UFPs giving peak 5 decay to smaller ones resulting in peaks 2, 3, and 4. This observation suggests that peak 5 originated from Al ions located in the inner part of the particles (volume ion). High speed MAS–NMR of bulk AlF_3 with a sample-spinning rate of 8.1 kHz exhibits a line at −16 ppm with a width of 2.1 kHz accompanied by strong side bands (Figure 7). This chemical shift position is exactly the same as that of peak 5 confirming the above assignment of the latter to volume ions. A comparison of Figure 4 (parts b and c) with Figure 7 demonstrates the effectiveness of the UFP NMR method for solid-state studies.

Line Width and Particle Size. In an AlF_3 crystal, each of the ^{27}Al nuclear spins interacts with a dipole field produced by six ^{19}F nuclear spins which is much stronger than that experienced by ^{27}Al nuclei in an $AlCl_3$ crystal (cf. Figure 2). The critical

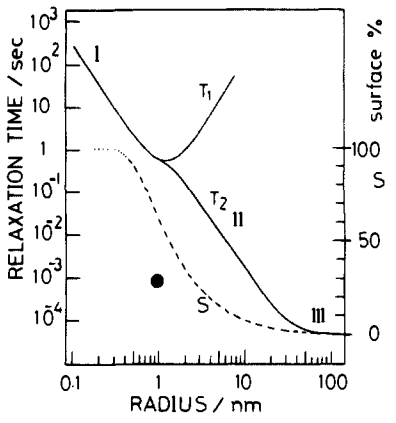

Figure 8. Size dependence of the calculated T_1 and T_2 of the AlF_3 UFP/methanol colloidal system at room temperature, where only dipole–dipole interactions between ^{27}Al and six neighbor ^{19}F nuclei are considered. The observed line width of peak 3 (Figure 4) were dotted in the figure assuming that the diameter of particles providing peak 3 is 2 nm. Surface fractions were illustrated in a dashed line. The diagram is divided in three regions: I, microscopic (molecular) region; II, mesoscopic (UFP) region; and III, macroscopic (solid) region.[9]

particle size at which narrowing takes place was estimated by calculating the NMR line width assuming a particle making random motion under the dipolar field. Following Debye's theory of dielectric dispersion,[7] the rotational correlation time for a spherical particle undergoing Brownian motion can be expressed as

$$\tau = 4\pi\eta a^3/(3kT) \quad (1)$$

where a is the radius of a particle, and other symbols have their usual meanings. On the other hand, T_2 of the nucleus I undergoing dipole–dipole interaction with a heterogeneous nucleus S (with spin number S) can be expressed[8] as

$$1/T_2^{\mathrm{I}} = \gamma_{\mathrm{I}}^2\gamma_{\mathrm{S}}^2\hbar^2 S(S+1)\left\{\frac{1}{6}J_0(0) + \frac{1}{24}J_0(\omega_{\mathrm{I}} - \omega_{\mathrm{S}}) + \frac{3}{4}J_1(\omega_{\mathrm{I}}) + \frac{3}{2}J_1(\omega_{\mathrm{S}}) + \frac{3}{8}J_2(\omega_{\mathrm{I}} + \omega_{\mathrm{S}})\right\} \quad (2)$$

where γ_{I} and γ_{S} denote the respective gyromagnetic ratios and $J_i(\omega)$ ($i = 0 \sim 2$), a Fourier transform of the correlation function of motions with a frequency ω. For rotational motions J_i can be written as

$$J_0(\omega) = 24/(15r^6)[\tau(1 + \omega^2\tau^2)]$$
$$J_1(\omega) = 4/(15r^6)[\tau(1 + \omega^2\tau^2)]$$
$$J_2(\omega) = 16/(15r^6)[\tau(1 + \omega^2\tau^2)] \quad (3)$$

where r denotes the distance between nuclei I and S. From eqs 1–3, T_2^{I} can be described as a function of the size of a particle. Figure 8 shows the T_2^{Al} curve for AlF_3 UFPs dispersed in methanol at room temperature.[9] It can be seen that motional narrowing occurs at a critical diameter of ca. 60 nm, and UFPs with a diameter less than 1 nm satisfy the extreme narrowing condition. The observed line width (FWHM), 7.2 kHz, is in reasonable agreement with the value obtained from the calculation of second moment (6.8 kHz) including only dipole–dipole interaction. With use of this figure, a mesoscopic region can be defined from the standpoint of NMR as the size region where motional narrowing occurs. In the figure, microscopic (molecular NMR region), mesoscopic (UFP NMR region), and macroscopic (bulk NMR region) regions are demonstrated.

The observed line widths of peaks 3 and 4 are considerably different from calculated ones plotted in Figure 8, which suggests that quadrupole interaction is predominant for the line width of AlF_3 UFPs. The calculated line width of UFPs with 2-nm diameter is less than 1 Hz from Figure 8. The observed line width of peak 3 (viz. 417 Hz) is, therefore, substantially due to quadrupole interaction. Accidentally, the value 417 Hz from quadrupole interaction coincides with the difference between the observed line width (including dipole–dipole and quadrupole interactions)/the width of bulk sample, 7.2 kHz, and of the calculation taken into account only for dipole–dipole interaction, 6.8 kHz. The case is the same for peak 5 arising from the larger UFPs. For UFPs with a diameter of 10 nm, the line width calculated on the assumption of only dipole–dipole interaction is 26.5 Hz which is 2.7% of the observed line width roughly estimated from Figure 4b.

The broadening of peak 1 assigned to ions in methanol is attributable to the variation of ionic species. Four kinds of complex ions, $Al^{3+}F^-_n$ ($n = 1 \sim 4$) are reported in an aqueous solution of $AlF_3{\cdot}9H_2O$.[10] In addition, because of low symmetric structure of $Al^{3+}F^-_n$ complex ions, quadrupole interactions would also be quite effective in broadening the lines.

The UFPs in a size region in which motional narrowing is expected to occur are characterized by a large portion of surface atoms to inner ones. The fraction of surface ions is also plotted in Figure 8 as a dashed line against the size of the particles, where the UFP is approximated by a sphere with a certain radius and the surface by a spherical shell with uniform thickness of 0.27 nm (diameter of a fluorine ion). With decreasing particle size, the increase in surface fraction is found to be parallel to T_2. More than 60% of the ions are expected to be at the surfaces of UFPs with a diameter of 2 nm which is comparable to the size of UFPs giving rise to peaks 2, 3, and 4. Peak 3 is also observable from the fraction NP100 as a minor peak (Figure 4b). It can, therefore, be reasonably interpreted that peak 3 results from the surface nuclei.

For systems satisfying the extreme narrowing condition (i.e., when $\omega\tau \ll 1$), the ratio T_2/T_1 becomes unity. Such a condition is expected to be realized in the case of UFPs having a diameter smaller than ca. 1.0 nm ($\omega\tau$ is 0.04 for AlF_3 UFPs with a diameter of 1.0 nm). Since the experimental values of T_2/T_1 are 0.75 and 0.21 for the peaks 3 and 4, respectively, the lower limit of the diameter of UFPs in the fraction P100 is estimated to be larger than 1 nm. This estimation substantiates the results from ultrafiltration preparations and TEM observations.

Nature of Chemical Bonding and the Size of UFPs. An ideal bulk ionic crystal with closed shell electronic structure has a unique chemical shift. However in the UFP, as the particle size becomes smaller, the chemical shift changes to lower fields as is shown in Figure 4. The chemical shift of bulk AlF_3 powder, viz. −16 ppm (Figure 7), is exactly the same as that of the peak 5 resulting from the larger UFPs (ca. 10 nm). The chemical shifts of UFPs with size ranging from 1 to 3 nm are −5, −8, and −12 ppm, while the NMR signal from the complex ions is located at 10 ppm. The paramagnetic shifts due to decrease of the size of UFPs seem to reflect the change of the nature of chemical bonding around aluminum ions. It is observed that the ^{27}Al NMR chemical shift of aluminum halides is located in the lower field region with increase in the covalency.[11] Actually, an interplaner spacing of (011) reflection in X-ray diffraction of relatively large UFPs (NP100) is shortened by 1%. This finding strongly suggests an increase in covalency of the Al–F bonds of UFPs. Therefore XPS measurements were carried out to study the electronic state of chemical bonds in AlF_3 UFPs.

Auger parameters (APs), defined as the sum of the kinetic energy of Auger electrons and the binding energy of photoelectrons,[12] were investigated because AP has a simple physical

(7) Debye, P. *Polar Molecules*; Dover: New York, 1929; Chapter 5.
(8) Abragam, A. *The Principles of Nuclear Magnetism*; Oxford University Press: London and New York, 1961; Chapter 8.
(9) There is an inadequate description in Figure 1 of ref 1 concerning the size dependence of T_1 and T_2. The notation of the abscissa which is described as the diameter should be read as radius. See, also: Kimura, K.; Satoh, N. *Chem. Lett.* **1989**, 1317.

(10) Matwiyoff, N. A.; Wageman, W. E. *Inorg. Chem.* **1970**, *9*, 1031–1036.
(11) O'Reilly, D. E. *J. Chem. Phys.* **1960**, *32*, 1007–1012.

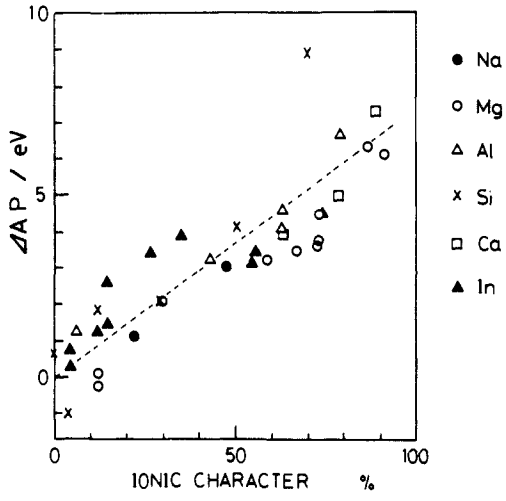

Figure 9. Chemical shifts of Auger parameter (AP) plotted against the ionicity (*I*) of the compounds. All values of AP were cited from ref 16.

meaning as the extra/atomic relaxation energy, which is sensitive to the character of the chemical bonds. Secondly, AP is unaffected by a charge-up process so that absolute values can be compared between different insulating samples with high accuracy.[12-15] When the chemical shifts of AP of authentic compounds[16] are plotted against Pauling's ionic character (*I*) for various bielement compounds (cf. Figure 9), it is observed that the chemical shift of AP is a monotonously decreasing function[17] of *I*. Further, all shifts from the authentic samples are in the same range. The APs are found to change from 0 to ca. 7 eV with an increase in *I* from 0 to 0.9. The change of ionicity of UFPs, therefore, can be estimated from the change of AP. APs of fluorides have high sensitivity for XPS, and those corresponding to the Auger line $KL_{23}L_{23}$ and of 1s photoelectrons of fluorine (AP_Fs) of AlF_3 bulk, NP100 UFP, and P100 UFP samples are found to be 1339.20, 1339.55, and 1340.00 eV, respectively (Figure 10). The difference of AP_F between bulk and P100 UFPs corresponds to that of *I* from 0.92 to 0.88. These changes of AP_F of UFPs are presumably underestimated because of recrystallization from free ions during the deposition process of colloidal solutions. The surfactant-treated AlF_3 UFPs show the smallest ionic character as 0.84 (not shown in the figure) in which the recrystallization process is suppressed. These results from XPS measurements are consistent with those from NMR.

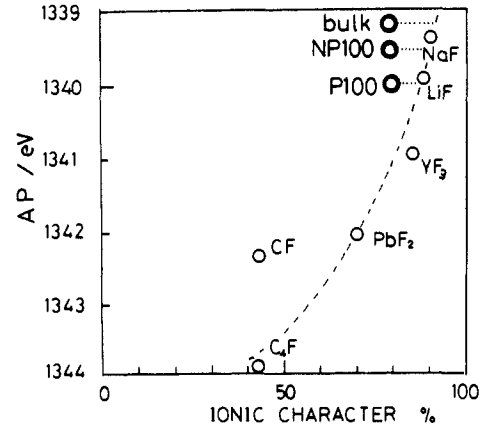

Figure 10. Chemical shifts of fluorine Auger parameter plotted against the ionicity of the compound. The values of APs except for AlF_3 bulk and UFPs were cited from ref 16.

The increase of covalency with the decrease of size of UFPs is not completely explainable at the present time. Increase of the number of surface ions, coordination numbers of which are smaller than those of bulk ions, seems to be one of the causes for this change. Tsukada et al. have calculated the electronic structure of the vertex, edge, plane, and bulk of magnesium oxide cluster with a DV-S_α method[18] and showed that covalencies increase and Mulliken charges of ions decrease in the order from bulk to vertex. These changes are understood as a result of the reduction of electrostatic contributions to the stabilizing energy of a crystal induced by the decrease of the coordination number at surfaces. Their results explain the fact that the NMR signal from the surfaces (peak 3 of Figure 4) is located in a lower field than that of bulk signal (peak 5).

The present authors believe that UFP NMR is one of the available techniques of high-resolution solid-state NMR including proton NMR and other kinds of nucleus and that UFP NMR will be more general in combining with the more refined techniques for preparing UFPs and their dispersions.

Acknowledgment. We thank Dr. K. Deguchi (Akishima Branch of JEOL Co. Ltd.) and Dr. M. Hashimoto (Tochigi Institute of Kao Co. Ltd.) for the measurements of high-resolution ^{27}Al MAS NMR of bulk AlF_3. We also thank S. Bandow for helpful discussions and suggestions and Dr. L. S. Prabhu Mirashi for careful reading of the manuscript.

(12) Wagner, C. D. *Anal. Chem.* **1975**, *47*, 1201-1203.
(13) Wagner, C. D. *Faraday. Disc. Chem. Soc.* **1975**, *60*, 291-300.
(14) Kuroda, H.; Ohta, T.; Sato, Y. *J. Electron Spectrosc. Relat. Phenom.* **1979**, *15*, 21-26.
(15) West, R. H.; Castle, J. E. *Surf. Interface Anal.* **1982**, *4*, 68-75.
(16) Wagner, C. D.; Riggs, W. M.; Davis, L. E.; Moulder, J. F. *Handbook of X-ray Photoelectron Spectroscopy*: Muilenberg, G. E., Ed.; Perkin-Elmer Co. Ltd.: 1978.
(17) Firemans, L.; Hoogewijs, R.; Vennik, J. *Surf. Sci.* **1975**, *47*, 1-40.
(18) Tsukada, M.; Adachi, H.; Satoko, C. *Prog. Surf. Sci.* **1983**, *14*, 113-174.